

Adjustable optical anisotropy in porous GaAs

Vladimir Kochergin^{a)} and Marc Christophersen
Lake Shore Cryotronics, Inc., Columbus, Ohio 43082

Helmut Föll

Materials Science, Faculty of Engineering, University of Kiel, Kaiserstrasse 2, 24143 Kiel, Germany

(Received 25 May 2004; accepted 23 November 2004; published online 19 January 2005)

We report a theoretical investigation of the optical properties of porous (100) GaAs having crystallographic pores. An effective medium approach is used for the calculations. A biaxial anisotropy of the material is predicted for most of the material parameters. The parameter windows for different kinds of uniaxial anisotropy are predicted as well. It is shown that the type and value of the optical anisotropy, and even the direction of the optical axes, can be controlled by GaAs etching parameters, and this letter gives the theoretical blueprint for the overall pore morphology required for that. © 2005 American Institute of Physics. [DOI: 10.1063/1.1849846]

Porous semiconductors¹ (Si, Ge, InP, GaP, GaAs, GaN, etc.) have attracted much attention recently since they allow one to engineer optical properties^{2,3} in a relatively simple way. Such materials are usually formed by electrochemical etching of the nonporous semiconductors in some special electrolytes. Optical applications of such materials are predicted to be wide.^{4–6} Although the research has been mainly devoted to the isotropic properties of porous semiconductors, it was shown recently^{7–10} that mesoporous Si etched on (110)-oriented substrates exhibits uniaxial behavior with the optical axis in the plane of the film (coinciding with the <001> crystallographic direction). A remarkable result is that in the infrared spectral range such a “metamaterial” offers larger values of the optical birefringence than any commonly known natural materials while being highly transparent at these wavelengths.

Here we present a theoretical analysis of the porous GaAs material^{11–13} etched on (100)-oriented substrate, based on the effective medium approach (EMA). This method is capable of analyzing complex, multiple pore-lattice materials with noncircular cross sections of the pores. In this context the porous GaAs is treated as macroscopically homogeneous and is assigned an effective dielectric permittivity tensor.

The crystallographically oriented pores in porous GaAs grow preferentially in the <111>B crystallographic direction. The zinc-blende lattice of the III–V compounds consists of double layers with alternating short (three bonds) and long (one bond) distances, occupied by A (Ga) or B (As) atoms. The <111>B direction runs from B to A layers along the shortest distance between A and B planes (or from B to A along the longest distance between the A and the B planes). A planes are generally more stable against electrochemical dissolution than B planes. The <111>A directions can be represented as $-Ga \equiv As - Ga \equiv As -$, while <111>B can be represented as $-As \equiv Ga - As \equiv Ga -$ (–means one bond¹³). For an (100)-oriented GaAs wafer, pores thus grow along four <111> directions. The number of <111>B directions in the pore lattices depends on the nucleation conditions for the pores. Two types of pore nucleation have been observed:¹⁴ uniform and nonuniform nucleation. Nonuniform nucleation usually resulted in the formation of “pore domains” on the surface of

the sample consisting of more or less equally distributed <111>-oriented pores. For uniform nucleation the majority of the pores grow just in the two <111> directions going “downwards,” while the “upward” pair of <111> directions is suppressed. Figures 1(a) and 1(b) show SEM images of the pores in GaAs obtained at uniform and nonuniform nucleation conditions (note the triangular cross section of the pores in GaAs).

In our model the following assumptions are made: (1) porous GaAs material can be represented by four sublattices of air voids in the bulk of GaAs such that the air voids in each sublattice have their axes essentially parallel to each other; (2) the bulk GaAs is isotropic and has the dielectric permittivity ϵ_{GaAs} ; (3) the pores are spatially separated and affect each other only through the depolarization factor (this limits the validity of the used method to relatively small porosities); (4) the wavelength of electromagnetic wave considerably exceeds the pore cross section.

The electromagnetic wave with the electric field vector \mathbf{E} in the porous GaAs gives rise to the displacement vector $\mathbf{D} = \epsilon_{GaAs} \mathbf{E} + \mathbf{P}$, where \mathbf{P} is the effective polarization of all the pores in a unit volume. The effective dielectric permittivity tensor $\hat{\epsilon}^{(eff)}$ is defined according to $\mathbf{D} = \hat{\epsilon}^{(eff)} \mathbf{E}$. According to the listed assumptions, $\mathbf{P} = \sum_{i=1}^4 \mathbf{P}^{(i)}$, where $\mathbf{P}^{(i)}$ is the polarization of the i th sublattice. Hence,

$$\hat{\epsilon}^{(eff)} \mathbf{E} = \epsilon_{GaAs} \mathbf{E} + \sum_{i=1}^4 \tilde{\mathbf{P}}^{(i)}. \quad (1)$$

The polarization of each pore in the i th sublattice is a linear function of the local electric field “seen” by each pore

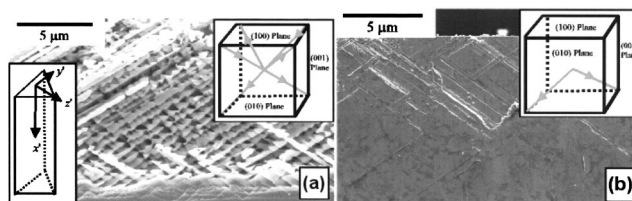


FIG. 1. (a), (b) SEM images of the porous GaAs layer with crystallographic pores; (c) the schematic drawing showing the pore lattices accounted for by the model for the case of porous GaAs electrochemically etched on (100) oriented substrates, and (d) the coordinate system associated with the pore lattice.

^{a)}Electronic mail: vkochergin@lakeshore.com

$\mathbf{E}_L^{(i)} : \mathbf{P}^{(i)} = N^{(i)} \hat{\alpha}^{(i)} \mathbf{E}_L^{(i)}$, where $N^{(i)}$ is a number of the pores in a unit volume, $\hat{\alpha}^{(i)}$ is the polarizability tensor of each pore. For arbitrary shaped inclusions¹⁵ $\mathbf{E}_L^{(i)} = \mathbf{E} + (\bar{\mathbf{L}}^{(i)} \cdot \bar{\mathbf{P}}^{(i)}) / \varepsilon_{\text{GaAs}}$, where $\bar{\mathbf{L}}^{(i)}$ is the depolarization factor. $\hat{\alpha}^{(i)}$ is a tensor diagonalizable in the coordinate system in which one of the axes coincides with the pore growth direction. If a coordinate transformation matrix $\hat{\mathbf{A}}^{(i)}$ is introduced between the reference coordinate system and the coordinate system of i th sublattice, the polarization of the i th sublattice in the reference coordinate system is

$$\bar{\mathbf{P}}^{(i)} = \varepsilon_{\text{GaAs}} \hat{\mathbf{A}}^{(i)} \hat{\mathbf{M}}^{(i)} \hat{\mathbf{A}}^{(i)-1} \bar{\mathbf{E}}^{(i)} \quad (2)$$

where $\hat{\mathbf{M}}_{j,j}^{(i)} = (N^{(i)} \alpha_{j,j}^{(i)}) / (\varepsilon_{\text{GaAs}} - L_{j,j} N^{(i)} \alpha_{j,j}^{(i)})$, $j=1,2,3$; and $\hat{\mathbf{M}}_{j,k}^{(i)} = 0$, if $j \neq k$.

We will follow the approach of Maldovan,¹⁶ who applied the internal field approach combined with finite element method to find the polarizability tensor elements for the inclusions with triangular shape: The dipole moment \mathbf{p} of the air-filled pore in GaAs is defined as the product of $\hat{\alpha}^{(i)}$ and \mathbf{E}_L . Under the approximation of a single pore in an infinite medium the local field \mathbf{E}_L and external field \mathbf{E} can be shown to be the same,²² so $\mathbf{p} = (1 - \varepsilon_{\text{GaAs}}) V (\int \bar{\mathbf{E}}_{\text{int}} dV / V)$, where the integration is performed within the pore. If β is defined as integral of the internal electric field over the pore volume divided by pore volume and the external field value, in the case of electric field alignment along the axis j of the coordinate system associated with the i th sublattice, the dipole moment is $\mathbf{p}_j^{(i)} = (1 - \varepsilon_{\text{GaAs}}) V \beta_j^{(i)} \mathbf{E}_{\text{ext},j}$. β is thus independent of pore volume and the external electric field and relates the effect of the particle shape on the electric field; it can be determined numerically. By replacing α_i in Eq. (2) by $(1 - \varepsilon_{\text{GaAs}}) V \beta_i$, one obtains:

$$\hat{\varepsilon}^{(\text{eff})} = \varepsilon_{\text{GaAs}} \left[\hat{\mathbf{I}} + \sum_{i=1}^4 \hat{\mathbf{A}}^{(i)} (\tilde{\mathbf{M}}^{(i)}) \hat{\mathbf{A}}^{(i)-1} \right], \quad (3)$$

where $\tilde{\mathbf{M}}_{j,j}^{(i)} = [f_i (1 - \varepsilon_{\text{GaAs}}) \beta_j^{(i)}] / [\varepsilon_{\text{GaAs}} - L_{j,j} f_i (1 - \varepsilon_{\text{GaAs}}) \beta_j^{(i)}]$, $j=1,2,3$; and $\tilde{\mathbf{M}}_{j,k}^{(i)} = 0$, if $j \neq k$, where $\hat{\mathbf{I}}_{i,j} = \delta_{i,j}$, and f_i is the ‘‘porosity’’ of i th pore lattice, $\sum_{i=1}^4 f_i = p$, $0 < p < 1$, where p is the porosity of the porous GaAs.

Let us introduce the reference coordinate system such that X and Y axes are directed toward two of $\langle 011 \rangle$ crystallographic directions, OZ direction coincides with $\langle 100 \rangle$ direction, and the pore-lattice coordinate system as shown in the left insert in Fig. 1(a) for each of the pore lattices. The transformation matrices can be found from geometrical considerations. To understand the effect of the triangular shape of the pores on the optical anisotropy of the porous GaAs, let us calculate first the dielectric permittivity tensor as if the pores had circular cross section. In this case,¹⁷ $\beta_{22} = \beta_{33}$ and $L_{22} = L_{33} = (1 - L_{11})/2$,

$$L_{11} = \frac{x^2}{(1 - x^2)^{3/2}} [\text{arctch}(\sqrt{1 - x^2}) - \sqrt{1 - x^2}],$$

where x the ratio between the axes length

$$x = c/a \quad (a > b = c),$$

$$\beta_{11} = \frac{\varepsilon_{\text{Si}}}{\varepsilon_{\text{Si}} - (\varepsilon_{\text{Si}} - 1)L_{11}},$$

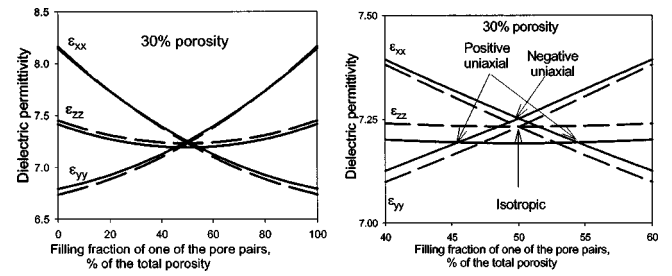


FIG. 2. Numerically calculated dielectric tensor elements of the porous GaAs with crystallographic pores etched on $\langle 100 \rangle$ -oriented substrate as a function of the relative filling fraction of one of the pore lattice pairs: (a) general view; (b) magnified view near the 50% filling fraction. The overall porosity of the sample is 30%. Dashed lines indicate the results of calculations for the case of the pores with circular cross section, solid lines indicate the results of calculations taking into account the triangular cross sections of crystallographic pores in GaAs.

$$\beta_{22} = \beta_{33} = \frac{2\varepsilon_{\text{Si}}}{2\varepsilon_{\text{Si}} - (\varepsilon_{\text{Si}} - 1)(1 - L_{11})}.$$

The pores in GaAs are best represented as cylinders [see Figs. 1(a) and 1(b)], or as the limiting case of ellipsoids with $x \rightarrow 0$.

The results of calculations are presented in Fig. 2 (dashed lines). The electromagnetic wave was assumed to propagate along $\langle 100 \rangle$ direction with electric field vector coinciding with the $\langle 011 \rangle$ direction. A 30% porosity of the GaAs is assumed. Calculations show that a porous GaAs would exhibit a biaxial anisotropy for all relative filling fractions of two pore lattice pairs except for the case of equal filling, where it would behave as an optically isotropic material.

To take into account the triangular cross section of the pore we need to reevaluate the values of L_{ij} and β_i . Since the ratio of pore length to pore cross section for porous GaAs is very high, $L_{11} = 0$ and $\beta_{11} = 1$. For equilateral triangular shape inclusions¹⁷ $L_{22} = 0.5 \Rightarrow L_{33} = 1 - L_{22} = 0.5$. In our calculations the β_2 was assumed to be 1.82, while $\beta_3 = 1.86$.

These corrections account for the triangular shape of the pore cross sections and allow calculations of the dielectric permittivity tensor elements of porous GaAs with the same set of parameters as used for the calculations for the circular pore cross section. The results of such calculations are also presented in Fig. 2. The triangular shape of the pore causes interesting effects, which can be viewed better in Fig. 2(b): For pore lattice pairs with identical representation or ‘‘weight,’’ i.e., a relative filling fraction of 50%, porous GaAs no longer exhibits isotropic behavior, but rather becomes a negative uniaxial crystal with an optical axis that coincides with the $\langle 100 \rangle$ direction. Besides the case of both pore lattice pairs being equally represented, two more points of nonbiaxial behavior appear. For the parameters of the porous GaAs as used for the calculations, these points correspond to filling fractions of roughly 45.5% and 54.5%. At these points the porous GaAs will exhibit positive uniaxial behavior with optical axes aligned along the two perpendicular $[011]$ directions, respectively. In all other cases the porous GaAs will exhibit biaxial behavior. Hence, porous GaAs provides the unique capability to control not only the optical anisotropy value, as, for example, in mesoporous Si etched on $\langle 110 \rangle$ oriented substrates,^{18,7-10} but also the optical anisotropy type (uniaxial or biaxial), and even the direction of the optical axis by modifying the etching parameters.

The challenge is to develop the right filling factors of the pore lattices of the porous GaAs for the desired optical properties by finding the proper electrochemical etching conditions. Beside electrolyte composition, current density, or etching bias, the nucleation process plays a critical role for the overall morphology. Unlike the case of porous Si, pores in GaAs can nucleate in form of pore-domains or homogeneously on the surface. The pores in both cases are crystallographic (propagate along $\langle 111 \rangle_B$ directions) and from one primary nucleation point on the (100) surface two primary crystallographic pores start to grow. If the nucleation points are dense enough, no branching of the pores is observed, and a uniform three-dimensional structure will develop. However, if the nucleation points are less dense, multiple branching of the two initially nucleated pores and of the secondary pores created by branching will occur, the result is a pore domain with a particular structure. For a homogeneous nucleation it is necessary to obtain a high density of nucleation points on the surface of the sample, which can be arrived at by a two-step anodization process.²⁰ Filling factor other than 50% might be obtained by starting with a substrate that is slightly off the (100) orientation, because the growth direction more steeply inclined is often favored in pore growth. Further details on the porous GaAs fabrication can be found elsewhere.^{1,21}

In conclusion, EMA was applied to calculate the optical anisotropy of porous GaAs etched on (100) oriented substrate with crystallographic pores. It was predicted that porous GaAs would exhibit biaxial anisotropy except for three narrow ranges of layer parameters, where it will exhibit negative uniaxial anisotropy with optical axis aligned with one of [011] crystallographic directions or positive uniaxial anisotropy with an optical axis that coincides with the $\langle 100 \rangle$ crystallographic direction. Such a material not only will exhibit biaxial optical anisotropy for some of the anodization parameters (unlike the case of porous Si which exhibits either isotropic or uniaxial behavior for all common substrate orientations), but also gives the opportunity to control the type and value of optical anisotropy and even the direction of

the optical axes through the tuning of anodization parameters. The well-known optical effects common to biaxial crystals, such as conical refraction, should be observable in porous GaAs.

- ¹H. Föll, S. Langa, J. Carstensen, M. Christophersen, and I. M. Tiginyanu, *Adv. Mater. (Weinheim, Ger.)* **15**, 183 (2003).
- ²A. Birner, R. B. Wehrspohn, U. M. Gösele, and K. Bush, *Adv. Mater. (Weinheim, Ger.)* **13**, 377 (2001).
- ³I. M. Tiginyanu, I. V. Kravetsky, S. Langa, G. Marowsky, J. Monecke, and H. Föll, *Phys. Status Solidi A* **197**, 549 (2003).
- ⁴G. Vincent, *Appl. Phys. Lett.* **64**, 2367 (1994).
- ⁵V. Pellegrini, A. Tredicucci, C. Mazzoleni, and L. Pavesi, *Phys. Rev. B* **52**, 14328 (1995).
- ⁶V. Kochergin, *Omnidirectional Optical Filters* (Kluwer Academic, Boston, 2003).
- ⁷D. Kovalev, G. Polisski, J. Diener, H. Heckler, N. Künzner, V. Yu. Timoshenko, and F. Koch, *Appl. Phys. Lett.* **78**, 916 (2001).
- ⁸J. Diener, N. Künzner, D. Kovalev, E. Gross, and F. Koch, *J. Appl. Phys.* **91**, 6704 (2002).
- ⁹J. Diener, N. Künzner, E. Gross, D. Kovalev, and M. Fujii, *Opt. Lett.* **29**, 195 (2004).
- ¹⁰Q. H. Wu, L. De Silva, M. Arnold, I. J. Hodgkinson, and E. Takeuchi, *J. Appl. Phys.* **95**, 402 (2004).
- ¹¹S. Langa, J. Carstensen, I. M. Tiginyanu, M. Christophersen, and H. Föll, *Electrochem. Solid-State Lett.* **5**, C14 (2002).
- ¹²B. H. Erne, D. Vanmaekelbergh, and J. J. Kelly, *J. Electrochem. Soc.* **143**, 305 (1996).
- ¹³P. H. L. Notten, J. E. A. M. van den Meerakker, and J. J. Kelly, *Etching of III-V Semiconductors: An Electrochemical Approach* (Elsevier Science, Oxford, 1991).
- ¹⁴S. Langa, J. Carstensen, M. Christophersen, H. Föll, and I. M. Tiginyanu, *Appl. Phys. Lett.* **78**, 1074 (2001).
- ¹⁵A. D. Yaghjian, *Proc. IEEE* **68**, 248 (1980).
- ¹⁶M. Maldovan, M. R. Bockstaller, E. L. Thomas, and W. C. Carter, *Appl. Phys. B: Lasers Opt.* **76**, 877 (2003).
- ¹⁷L. D. Landau and E. M. Lifshits, *Electrodynamics of Continuous Media*, 2nd ed. (Butterworth-Heinemann, Oxford, 1984).
- ¹⁸J. Diener, N. Künzner, D. Kovalev, E. Gross, V. Yu. Timoshenko, G. Polisski, and F. Koch, *Appl. Phys. Lett.* **78**, 3887 (2001).
- ¹⁹P. Schmuki and L. E. Erickson, *Appl. Phys. Lett.* **73**, 2600 (1998).
- ²⁰P. Schmuki, D. J. Lockwood, H. J. Labbe, and J. W. Fraser, *Appl. Phys. Lett.* **69**, 1620 (1996).
- ²¹H. Föll, S. Langa, J. Carstensen, S. Lölkes, M. Christophersen, and I. M. Tiginyanu, *III-Vs Rev.* **16**, 42 (2003).
- ²²A. Shivola and I. V. Lindell, *J. Electromagn. Waves Appl.* **3**, 37 (1989).